

Flow properties of hydroxypropyl guar gum and its long-chain hydrophobic derivatives

Romano Lapasin, Lorenzo De Lorenzi, Sabrina Pricl & Giovanni Torriano*

Department of Chemical, Environmental and Raw Materials Engineering - DICAMP, University of Trieste, Piazzale Europa 1, I-34127 Trieste, Italy

(Received 7 July 1995; revised version received 2 October 1995; accepted 9 October 1995)

This paper deals with the rheological properties under continuous shear flow conditions of aqueous systems of hydroxypropyl guar gum (HPG) and three derivatives, of the same or lower molecular weight (MW) than HPG, characterized by different contents of long-chain hydrophobic pendants. The shear-dependent behavior of HPG and of the derivative with low molecular weight and low degree of hydrophobization (LMLH) resembles that of isotropic polymer solutions; accordingly, it can be fairly well described by the Cross equation, the effect of temperature discussed in terms of activation energy for viscous flow and the dependence of the Cross parameters η_0 and λ on polymer concentration expressed by simple power-laws. The other two derivatives considered, i.e. the one of low MW and high long-chain hydrophobic substitution and the other of a MW as high as that of HPG and a low hydrophobic pendant content (LMHH and HMLH, respectively) show an unusual behavior, characterized by the existence of a shear rate interval in which the shear viscosity undergoes a catastrophic breakdown, and which cannot be described by any simple rheological model. Nevertheless, as far as the temperature effect is concerned, all experimental data can be combined into one master curve by a simple shifting procedure. All systems exhibit marked time-dependent properties of the thixotropic type, which are described with a stretched exponential model and discussed in terms of the variation of the model parameters with temperature and polymer concentration. The peculiar features of the long-chain hydrophobic derivatives can be ascribed to a balance between inter- and intramolecular interactions, which is mainly governed by the local stress field.

INTRODUCTION

In recent years, the study of polymer amphiphiles has seen a growing interest in the role these macromolecules play in biology and in their possible pharmaceutical, biotechnological and industrial applications (Shalaby *et al.*, 1991).

Biopolymers as well as synthetic charged and uncharged polymers have been used as the hydrophilic backbone of the amphiphilic macromolecule. Among all these water soluble polymers, naturally occurring or chemically modified polysaccharides show unique features, such as the formation of weak gel systems or polymeric liquid crystals (Yalpani, 1992; Lapasin & Pricl, 1995).

Guar gum is a galactomannan extracted from the seeds of *Cyamopsis tetragonoloba*, a native plant of India. As for many other polysaccharides, the ability of this biopolymer to undergo a wide range of chemical reactions provides an additional opportunity for an

expansion of its usage to many industrial sectors. Among the vast class of chemically modified products, a major role is played by hydroxypropyl guar gum (HPG), a hydrophobic derivative obtained from the native biopolymer via an irreversible nucleophilic substitution, using propylene oxide in the presence of an alkaline catalyst. HPG is currently used as a water blocking agent in the formulation of cartridge explosive, as a processing aid in the mining and mineral industry for the recovery and separation of some metals from their ores and as a slime depressant in froth flotation processes, in the preparation of workover and completion fluids for oil recovery operations, in the formulation of pastes for rotary screen textile printing and water-based paints (Lapasin & Pricl, 1995).

Hydrophobized polysaccharide derivatives which have long alkyl chains have been recently synthesized. Hydrophobic polysaccharide esters constitute a relatively new class of derivatives; they can be prepared from long-chain acid chlorides and notable examples are the *O*-palmitoyl derivatives of amylopectin and

*Author to whom correspondence should be addressed.

pullulan (Sunamoto *et al.*, 1985). Another important series of hydrophobic ether derivatives of polysaccharides can be obtained via irreversible nucleophilic substitution using aliphatic or aromatic halides, sulfates or epoxides. Representative examples here are the long alkyl chain products prepared from cellulose (Landoll, 1982), amylose, dextran and pullulan (Sunamoto *et al.*, 1984) and guar gum derivatives (Nicora *et al.*, 1990).

Both these classes of polysaccharide hydrophobic derivatives find a number of important applications (Lapasin & Pricl, 1995). Hydrophobic derivatization, for instance, offers a new route to chromatographic separation and hydroxypropyldextran derivatives have been prepared which, by virtue of their swelling in organic liquids, can be utilized in the separation of oils, lipids, hormones and fatty acids (Yalpani & Brooks, 1987). Another notable industrial application of these derivatives is in the formulation of pastes for rotary screen textile printing and water-based paints. In particular, hydrophobic modification of cellulose and guar gum derivatives such as HPG allows exploitation of intermediate molecular weight polymers, and their use as natural associative thickeners in the paint industry is growing steadily (Young & Fu, 1991; Kroon, 1993; De Lorenzi *et al.*, 1994).

Central to all possible applications of both HPG and its long-chain hydrophobic derivatives is the rheological behavior exhibited by their aqueous systems. Other formulations based on amphiphilic polymers of synthetic nature, such as hydrophobically modified ethylene oxide urethane rheology modifier (HEUR) and hydrophobically modified alkali swellable emulsion (HASE), have shown anomalous rheological properties, which have been interpreted in terms of the formation of a labile structural network, induced by the association of the hydrophobic groups (Glass, 1989; Reynolds, 1992; Mast *et al.*, 1993; Fonnum *et al.*, 1993); therefore, we can expect that similar mechanisms of association take place in hydrophobically modified HPG systems.

In spite of the industrially important applications and the relevant scientific interest, studies of the rheological behavior of such hydrophobized polysaccharide derivatives are scarce (Aubry & Moan, 1994). The aim of the present paper is a systematic investigation of the shear- and time-dependent properties of HPG and its long alkyl chain derivatives, and an evaluation of the effects of polymer concentration, degree of hydrophobic substitution and temperature on the rheological behavior of these systems.

MATERIALS AND METHODS

Materials

All the materials studied in this work were kindly supplied by Fratelli Lamberti S.p.A. (Albizzate, Italy).

The hydroxypropyl guar gum was prepared by alkaline etherification of guar gum with propylene oxide. The HPG obtained was characterized by a molar substitution of hydroxypropyl groups $MS \cong 1$ and a weight average molecular weight M_w of approximately 8×10^5 . HPG was subsequently etherified as such with docosylglycidylether in isopropylalcohol and in the presence of an alkaline catalyst, or after a controlled degradation to a lower molecular weight. Three different derivatives were thus obtained, having the following characteristics:

- HMLH: weight average molecular weight $M_w \cong 7 \times 10^5$, degree of substitution $DS = 0.00019$;
- LMHH: weight average molecular weight $M_w \cong 4 \times 10^5$, degree of substitution $DS = 0.00060$;
- LMLH: weight average molecular weight $M_w \cong 4 \times 10^5$, degree of substitution $DS = 0.00015$.

The molecular weights were determined by gel-permeation chromatography (Johnson & Porter, 1970), whereas the degree of substitution was determined by gas chromatography following the method suggested by Lee *et al.* (1983). All polymer aqueous systems were prepared by adding the proper amount of polymer to twice-distilled water under vigorous stirring. Once the polymer addition was complete, each system was left under stirring until the total dissolution of the polymer was achieved. The resultant solutions were left in the glass container to rest overnight before use.

The effect of polymer concentration C_p was investigated in the range 0.8–1.8% w/w, whereas the influence of temperature was monitored in the interval 5–55°C.

Apparatus and procedures

All rheological measurements were performed with two rotational rheometers, the Haake RV100 and RV20, both coupled with the measuring device CV100, mounted with a coaxial cylinder sensor system ZB15 (Couette type). The inner cylinder used with this coaxial sensor system has the following dimensions: 13.91 mm diameter, 32.30 mm length; the gap is 0.545 mm. During the tests, while the outer cap is driven, the inner cylinder is mechanically positioned and centered by an air bearing. The top and bottom surfaces of the inner cylinder are especially designed to minimize end effects. To prevent water evaporation during the tests, a thin film of silicone oil was applied to the edge of the aqueous solution.

Stepwise procedures were applied for the analysis of the shear- and time-dependent properties in continuous shear flow conditions. The multiple-step procedure consists of a sequence of different shear rates $\dot{\gamma}$, each shear rate being kept constant until a steady value of the shear stress τ_s is attained. The analysis of the shear-dependent properties can then be properly based upon the steady values of the shear stress obtained at the different shear rates, whereas the sequence of stress transients allows an inspection of the nature and extent

of the time-dependent properties to be performed. In the case of our polymers, only for HPG solutions could we reach a steady state value of the shear stress τ_s at the corresponding shear rate $\dot{\gamma}$ in reasonable times, whereas in the case of all long-chain hydrophobic derivatives, much longer times were required to reach steady state conditions. Practical operative conditions in these cases are given below.

Flow curves (shear stress vs shear rate plots) were fitted by using computerized non-linear regression analysis. In the on-off procedure, a shear rate is applied and kept constant until a steady value of the shear stress is attained, after which it is suddenly interrupted. After a given rest time t_r , the same stepwise variation of the shear rate is carried out. If the procedure is repeated for different rest times, and, accordingly, different stress transients are recorded, information on the time-dependent properties of the fluids and on their dependence on different rest times can be obtained. In the present work, all on-off tests were performed at constant $\dot{\gamma} = 3 \text{ s}^{-1}$.

RESULTS AND DISCUSSION

The application of the stepwise procedure allows an immediate distinction to be observed between the rheological properties of HPG and its long-chain hydrophobic derivatives. Indeed, whilst HPG exhibits almost negligible time-dependent properties in the entire range of shear rate explored (i.e., the shear stress transients are limited, confined within 1–2 min and the steady values of the stress τ_s are independent of the previous rheological history), a much more complex behavior is displayed by its hydrophobized derivatives. Figure 1 reports, as an example, the time-dependent behavior resulting from the application of a decreasing shear rate sequence on the derivative with the highest degree of hydrophobization and lower molecular weight (LMHH)

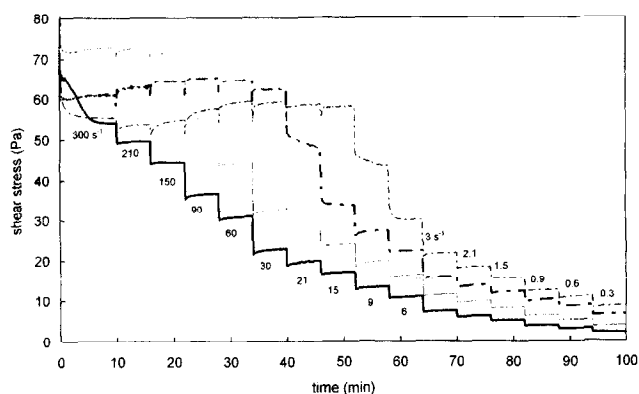


Fig. 1. Time-dependent behavior resulting from the application of a decreasing shear rate sequence ($\dot{\gamma}$ from 300 to 3 s^{-1}) on the LMHH system at $C_p = 1.2\%$ and at four different temperatures: $T = 5^\circ\text{C}$ (---), $T = 25^\circ\text{C}$ (- · - · -), $T = 45^\circ\text{C}$ (—) and $T = 55^\circ\text{C}$ (— — —).

at 5, 25, 45 and 55°C . As can be seen from this figure, at the highest shear rate applied, the system undergoes a strong stress decay, followed by a slight increase of the stress with time t . The subsequent transients are characterized by τ values increasing with increasing t , and the relevant steady values τ_s slightly increase with decreasing $\dot{\gamma}$. Further, at lower shear rates the stress manifests a catastrophic decay with time, again followed by transients which increase with time. This catastrophic decay of the stress appears to take place in a narrow critical shear rate region, which is a function of the temperature T . As T increases, this critical $\dot{\gamma}$ region shifts towards higher values, as can be inferred from the experimental data reported in Fig. 1. Quite analogous behaviors are observed at 15 and 35°C , but the relevant curves are not reported. At 15 and 35°C , the behavior of this system is quite similar, curves are not reported for the sake of plot readability. In terms of shear stress, this is equivalent to saying that a narrow band of the shear stress values exists, which is almost independent of temperature and within which a sharp transition of the rheological behavior under continuous flow conditions occurs. Indeed, for low values of τ , below the transition region, the rheological behavior can be described as shear-thinning, whereas above the upper limit of the transition region, the stress is only slightly dependent on the applied shear rate and, correspondingly, the shear viscosity η undergoes a catastrophic breakdown with increasing τ and ceases to be a unique function of the stress.

As regards the time scale of the stress transients, this is of the order of minutes for the lower and higher shear rate values applied, whereas in the shear rate range in which the catastrophic behavior is found, times up to 1 h are necessary to reach quasi-steady stress values. A more detailed picture of this catastrophic stress decay is shown in Fig. 2a, relative to the curve for LMHH at 45°C reported in Fig. 1. For small stepwise variations of the shear rate around the critical condition, we can observe a sigmoidal stress decay, which requires more than 1 h to level off (see Fig. 2a). This sigmoidal shape of the stress decay is maintained under different shear rate sequences applied, as evidenced in Fig. 2b.

All the above information concerns tests performed according to a decreasing shear rate sequence, that is from 300 to 0.3 s^{-1} . Quite analogous results were obtained by performing the stepwise tests according to the inverse sequence, i.e., from 0.3 up to 300 s^{-1} .

The other two long-chain hydrophobic polymers (HMLH and LMLH), which are characterized by almost the same degree of substitution of the hydrophobic pendants, manifest a time-dependent behavior, whose characteristics are intermediate between those of the LMHH and the HPG polymers, respectively. Also for these two systems, long times are required to reach a steady state of the stress in a region of intermediate values of the applied shear rate and, as we have seen for

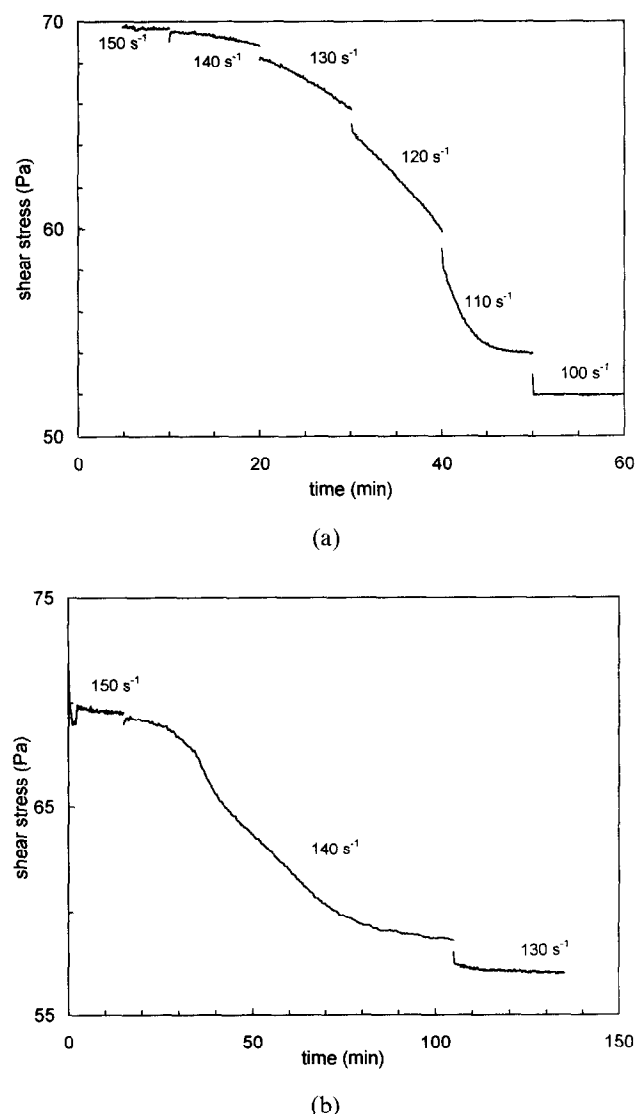


Fig. 2. Detailed picture of the stress decay relative to LMHH at $C_p = 1.2\%$, in the shear rate range (a) $\dot{\gamma} = 150\text{--}100\text{ s}^{-1}$; and (b) in a more restricted shear rate range ($\dot{\gamma} = 150\text{--}130\text{ s}^{-1}$).

the LMHH derivative, the steady value of τ may depend, sometimes to a considerable extent, upon the previous rheological history experienced by the system itself.

From the previous discussion we conclude that a standardized experimental procedure has to be adopted in order to determine reliable reference stationary values of the stress, upon which the subsequent analysis and comparison of the shear-dependent properties of all different systems can be based. Therefore, we selected to perform a decreasing shear rate sequence (see Fig. 1 for selected values of $\dot{\gamma}$ applied) in which the first $\dot{\gamma}$ value is kept constant for 10 min and all the remaining $\dot{\gamma}$ are maintained for 6 min, respectively.

By applying the procedure described above, we determined the stationary values of the stress τ_s for the HPG systems and the quasi-stationary values for all the long-chain hydrophobic derivatives. Accordingly, we

obtained the corresponding flow curves, which allowed us to distinguish between two different classes of shear-dependent behavior.

In fact, the shear-dependent behavior of the HPG and LMLH systems is quite similar to that exhibited by other isotropic polymer solutions and can be described, to a good approximation, with the Cross equation (Cross, 1965):

$$\eta = \eta_{\infty} + \frac{(\eta_0 - \eta_{\infty})}{1 + (\lambda \dot{\gamma})^n} \quad (1)$$

in which η_0 is the zero-shear rate viscosity (lower Newtonian plateau), η_{∞} is the infinite-shear rate viscosity (upper Newtonian plateau), λ is a characteristic time and n is a numerical exponent. Since, in our case, the experimental data seem to be far from approaching the second (upper) Newtonian region, we used a simplified version of equation (1) obtained by setting η_{∞} equal to the viscosity of water solvent at the corresponding temperature.

The values of the Cross parameters obtained for the HPG and LMLH systems with $C_p = 1.2\%$ from data fitting at all temperatures are reported in Table 1. As we can see from this table, for both systems n regularly decreases with increasing temperature, which indicates a weaker shear-dependence of viscosity in the power-law region at higher temperatures. η_0 for both systems decreases with increasing T according to an Arrhenius-type equation:

$$\eta_0 = A_0 \exp \frac{E_{\eta,0}}{RT} \quad (2)$$

The values of the pre-exponential factor A_0 and of the activation energy for viscous flow $E_{\eta,0}$ are 1.3×10^{-2} mPa s and 32.9 kJ/mol for the HPG system, and 3.2 mPa s and 18.9 kJ/mol for the LMLH system, respectively. For

Table 1. Values of Cross parameters (equation (1)) at different temperatures for the HPG and LMLH systems at $C_p = 1.2\%$

Polymer	T (°C)	η_0 (Pa s)	η_{∞} (mPa s) ^a	λ (s)	n
HPG	5	20.2	1.52	3.69	0.71
	15	12.0	1.14	2.25	0.70
	25	8.00	0.89	1.56	0.68
	35	5.28	0.72	1.04	0.67
	45	3.75	0.60	0.775	0.66
	55	2.15	0.50	0.411	0.64
LMLH	5	10.4	1.52	1.01	0.74
	15	8.64	1.14	0.834	0.72
	25	7.24	0.89	0.929	0.67
	35	5.65	0.72	1.00	0.63
	45	4.10	0.60	0.994	0.59
	55	2.96	0.50	0.812	0.57

T , temperature; η_0 , zero-shear rate viscosity; η_{∞} , infinite-shear rate viscosity; λ , characteristic time; n , numerical exponent. C_p , polymer concentration.

^a The infinite-shear rate viscosity values reported are the water viscosities at the corresponding temperature.

isotropic polymeric solutions, $E_{\eta,0}$ represents the maximum value of the activation energy, corresponding to the lower Newtonian plateau. Lower values are derived for the activation energy E_{η} , when the Arrhenius-type equation is used for correlating the viscosity values obtained for different temperatures at a given shear rate, far from the Newtonian plateau. Figure 3 shows that E_{η} regularly decreases with increasing shear rate for both the above systems, with a more marked decrease for the hydrophobic system LMLH.

The temperature dependence of the characteristic time, λ , for the HPG system can also be described by an Arrhenius type relationship. Contrarily, for the LMLM system, λ is nearly constant in the temperature range explored.

The shear-dependent behavior of the HPG and LMLH systems is qualitatively the same at the other concentrations examined, which evidently fall in the concentrated regime. In fact, as illustrated in Fig. 4, the concentration dependences of the Cross parameters η_0 and λ for both systems can be properly described with the power-law relationships characteristic of concentrated polymer solutions:

$$\eta_0 = aC_p^\alpha \quad (3)$$

$$\lambda = bC_p^\beta \quad (4)$$

The calculated values for the exponent α and β are 4.51 and 2.75, for the HPG system and 5.94 and 5.43 for the LMLH system, respectively. The α values are higher than those predicted for linear polymers interacting by purely topological entanglements ($\alpha = 3.75$) (de Gennes, 1979) and those obtained for hydroxyethyl guar gum solution with different molecular weight in concentrated regime ($\alpha = 4.16$) (Lapasin *et al.*, 1991). The behavior of these polymer systems can be traced to the formation of specific junctions between stiff, structurally regular chain sequences and of hydrophobic interactions between the long hydrocarbon pendants. A likely

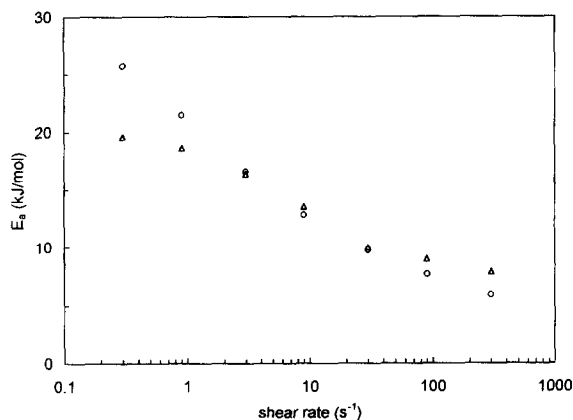


Fig. 3. Activation energy for viscous flow E_{η} vs shear rate $\dot{\gamma}$ for the HPG (Δ) and LMLH systems (\circ) at $C_p = 1.2\%$ and $T = 25^\circ\text{C}$.

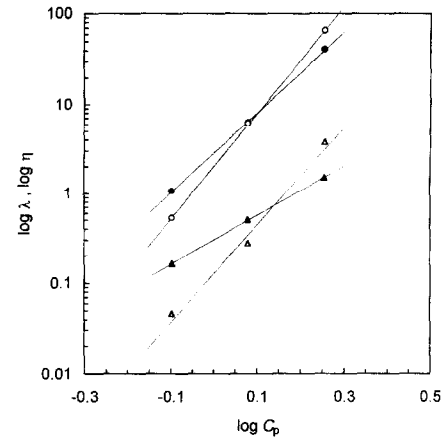


Fig. 4. Concentration dependence of the Cross parameters on polymer concentration for the HPG and LMLH systems at $T = 25^\circ\text{C}$. Experimental data: HPG: $\log \eta_0$ (Δ), $\log \lambda$ (\blacktriangle); LMLH: $\log \eta_0$ (\circ), $\log \lambda$ (\bullet). Lines: data fitting with equations (3) and (4).

explanation of the enhanced viscosity of these materials might, therefore, be that similar, though less stable, interactions occur in solution, in addition to physical entanglements of overlapping coils. This entanglement coupling, intensified by specific attractive forces, has the aptly descriptive name of hyperentanglements.

The shear-dependent behavior of the other two polymers (LMHH and HMLH) is undoubtedly more complex and cannot be easily described by a simple rheological model. This becomes evident when we compare the flow curves of all systems in a $\log \eta$ - $\log \tau$ plane, an example of which is reported in Fig. 5 for the four different systems at 25°C and at a polymer concentration $C_p = 1.2\%$. As we can see in this figure, the shear-dependent behavior of the polymer characterized by the highest degree of hydrophobization (LMHH) (and, to a minor extent, that of the long-chain derivative with higher molecular weight (HMLH)) is quite different from that exhibited by the other two

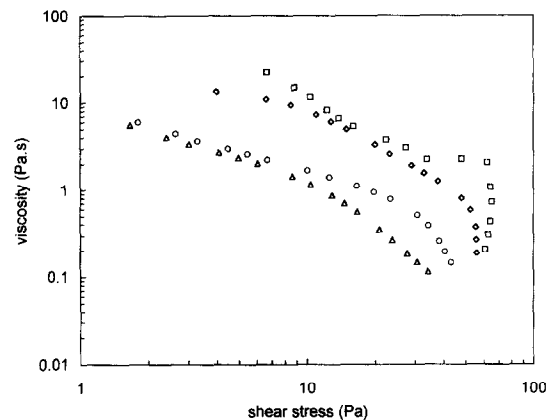


Fig. 5. Shear viscosity vs shear stress for the four different systems considered at $C_p = 1.2\%$ and $T = 25^\circ\text{C}$. (Δ), HPG; (\circ), LMLH; (\diamond), HMLH; (\square), LMHH.

polymers (HPG and LMLH), especially in the high stress region: here, the viscosity η of the LMHH system undergoes a sharp breakdown whereas the decay of η for HPG and LMLH systems follows a power-law, analogous to that observed for similar polymers in a wider range of stress values (Aubry & Moan, 1994).

As far as the temperature effect is concerned, we can say that the profiles of the shear viscosity η as a function of the shear stress τ remain qualitatively unchanged by changing T for both the HPG and the LMLH systems. For the other two systems (LMHH and HMLH), the similarity is strictly conserved in the temperature range 5–35°C; this provides the basis for combining all the experimental data into one master curve. In order to obtain the master curve for the viscosity function at an arbitrary reference temperature T_0 , from plots of $\log \eta$ vs $\log \tau$ for the different temperatures T , the curve at temperature T must be shifted along the viscosity and the shear stress axes in such a way that any regions of the T_0 curve and the shifted T curve superpose. Each superposition operation is determined by the two shift factors a_η and a_τ . In fact, the amounts by which $\eta(\dot{\gamma}, T)$ must be translated upward and to the right in order to achieve superposition are defined as $\log a_\eta$ and $\log a_\tau$. Thus, a single master curve can be obtained by plotting the reduced viscosity η_R vs the reduced shear stress τ_R , defined as:

$$\eta_R = \eta a_\eta \quad (5)$$

$$\tau_R = \tau a_\tau \quad (6)$$

Figure 6 shows the master curve obtained for the system LMHH with $C_p = 1.2\%$, having assumed 25°C as the reference temperature T_0 . The relevant values of the shift factors a_η and a_τ are reported in Table 2. The values of the stress shift factor are nearly independent of temperature, which implies that the viscosity breakdown

Table 2. Values of the shift factors for the master curves reported in Fig. 6

T (°C)	a_τ LMHH	a_η LMHH	a_τ HPG	a_η HPG
5	1.11	0.47	1.25	0.31
15	0.94	0.60	1.08	0.62
25	1.00	1.00	1.00	1.00
35	0.92	1.77	0.90	1.70
45	-	-	0.85	2.43
55	-	-	0.77	4.14

T , temperature; a_τ , a_η , shift factors.

takes place at the same critical stress in the temperature interval $T = 5$ –35°C. On the other hand, the dependence of the shift factor a_η on T follows an Arrhenius-type equation, as is generally expected for polymeric solutions. Finally, from Fig. 6 we can also observe that the master curve is far from approaching the lower Newtonian plateau in the experimental window explored. Figure 6 also gives the master curve for the HPG system with $C_p = 1.2\%$, having assumed 25°C as the reference temperature T_0 . The relevant values of the shift factors a_η and a_τ are reported in Table 2.

From all the above observations we can conclude that the shear-dependent behavior of these concentrated systems diverges from that of canonical polymeric solutions as the role played by the long-chain hydrophobic substituent increases. A sensible interpretation for the unusual properties of the hydrophobic systems can rely upon a distinction between three different flow regimes. In the low shear rate region, both inter- and intramolecular hydrophobic interactions exist, whose mutual balance depends on the specific features of the chains and the previous rheological history.

In the middle shear rate range, the flow field produces an appreciable orientation and stretching of the macromolecules, thus favoring the formation of an increased number of intermolecular hydrophobic interactions. This structural process reflects into a strong increase of the shear stress with increasing shear rate; this, in turn, leads to divergent rheological behaviors, especially in the case of the system with the highest degree of hydrophobization (LMHH). The same mechanism, essentially based on the change from primarily intramolecular to intermolecular associations caused by the flow field, has been invoked to explain the shear-thickening behavior observed in several synthetic associative polymers (Ballard *et al.*, 1988; Witten, 1988; Jenkins *et al.*, 1991).

The intermediate regime ends when the local shear stresses become high enough to overcome the constraints set by the hydrophobic interactions. Such a condition is reached in a very narrow stress interval, which does not depend on temperature; correspondingly, the shear viscosity undergoes a catastrophic breakdown, and the rheological behavior converges to that typical of entangled solutions.

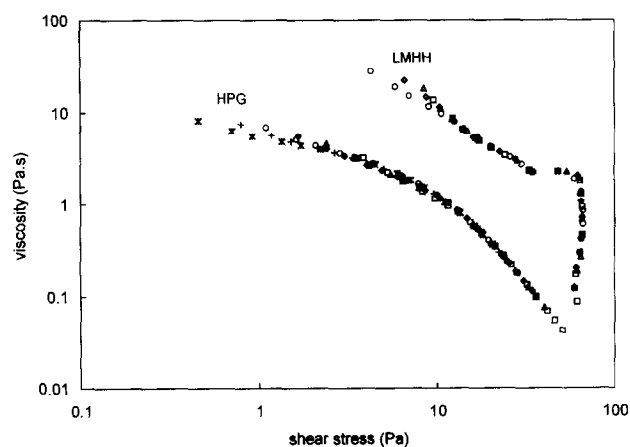


Fig. 6. Shear viscosity-shear stress master curves for the LMHH system with $C_p = 1.2\%$ and for HPG obtained assuming $T_0 = 25^\circ\text{C}$ and using the shift factors reported in Table 2. (\square), $T = 5^\circ\text{C}$; (Δ), $T = 15^\circ\text{C}$; (\diamond), $T = 25^\circ\text{C}$; (\circ), $T = 35^\circ\text{C}$; (+) $T = 45^\circ\text{C}$; (*), $T = 55^\circ\text{C}$.

The medium–low shear rate region is characterized by the presence of supermolecular structures within the systems, whose configuration strongly depends upon the kinematic conditions and the previous rheological history. This explains the difficulties encountered in the experimental determination of the equilibrium values of the corresponding shear stress. The same supermolecular structures are responsible for the marked time-dependent features and, in particular, for the thixotropic behavior of the long-chain hydrophobic materials. These latter properties can be highlighted by the application of the on–off procedure, whose objective is the evaluation of the amplitude and the kinetics of the thixotropic build-up process under rest conditions. As the rest time t_r increases, the initial stress overshoot increases and the characteristic time of the stress peak gradually shifts towards higher values. The stress overshoot ratio τ^* , defined as the ratio of the peak shear stress maximum and the stress equilibrium value at the corresponding shear rate is reported in Fig. 7 as a function of the rest time t_r for the four different systems at $C_p = 1.8\%$ and $T = 25^\circ\text{C}$. From Fig. 7 we can see that the structure rehealing process for the HPG and LMLH systems is limited and is almost completed within around 300 s, whereas much longer times are required to reconfigure the unperturbed state in the case of the LMHH and HMLH systems.

The extent and kinetics of the structural build-up process can be conveniently characterized by fitting the relevant $\tau^*(t_r)$ data with the following stretched exponential model:

$$\tau^* = \tau_{\infty}^* - (\tau_{\infty}^* - 1) \exp[-(t_r/t_{r,c})^m] \quad (7)$$

where t_r is the rest time, τ_{∞}^* is the asymptotic value of the stress overshoot ratio for $t_r \rightarrow \infty$, which measures the maximum extent of the structure rehealing process under rest conditions, $t_{r,c}$ is the critical rest time, necessary to partially remove shear history and to reconfigure the unperturbed state (to an extent equal to $1 - 1/e$), and m is

a parameter characterizing the build-up kinetics. All the other factors being the same, the recovery is faster in the initial rest time interval for lower m values. Tables 3 and 4 report the values of the adjustable parameters τ_{∞}^* , $t_{r,c}$ and m obtained from data fitting for different systems at different concentrations and temperatures.

From an inspection of Table 3 we can argue that the thixotropic recovery becomes remarkable and implies long rest times for the most concentrated hydrophobic systems with the highest degree of hydrophobization (LMHH) and molecular weight (HMLH). The structure rehealing process develops to lower extents at lower concentration and for increasing temperature, as we can see from the τ_{∞}^* values reported in Table 4. The thixotropic recovery is fast in the initial rest time interval for the HPG system (low m values), even if the delay times required to approach the final state are comparable with those derived for the other polymers. Finally, we can note that the influence of temperature on the kinetics of the process is quite different for the three systems examined. As T increases, the recovery becomes faster for the HPG and LMLH systems, whereas an appreciable increase of $t_{r,c}$ is observed for the LMHH system.

Table 3. Values of the parameters of the stretched exponential model (equation (7)) for the four different polymers considered at $C_p = 1.8\%$ and $T = 25^\circ\text{C}$

Polymer	τ_{∞}^*	$t_{r,c}$ (min)	m
HPG	1.18	0.18	0.32
LMLH	1.35	0.84	0.38
LMHH	1.72	1.91	0.64
HMLH	1.93	4.33	0.46

τ_{∞}^* , asymptotic value of the stress overshoot ratio for $t_r \rightarrow \infty$; $t_{r,c}$, critical rest time; m , parameter characterizing build-up kinetics.

Table 4. Values of the parameters of the stretched exponential model (equation (7)) for three different systems at $C_p = 1.2\%$

Polymer	T ($^\circ\text{C}$)	τ_{∞}^*	$t_{r,c}$ (min)	m
HPG	5	1.21	5.31	0.11
	15	1.15	4.31	0.13
	25	1.11	3.15	0.18
	35	1.08	2.43	0.24
	45	1.06	2.24	0.28
LMLH	5	1.19	2.20	0.38
	15	1.16	0.98	0.36
	25	1.13	1.88	0.39
	35	1.10	1.71	0.51
	45	1.04	1.90	0.92
LMHH	5	1.47	1.58	0.32
	15	1.41	2.99	0.29
	25	1.31	3.84	0.26
	35	1.24	4.66	0.27
	45	1.16	5.90	0.30

For abbreviations see Table 3.

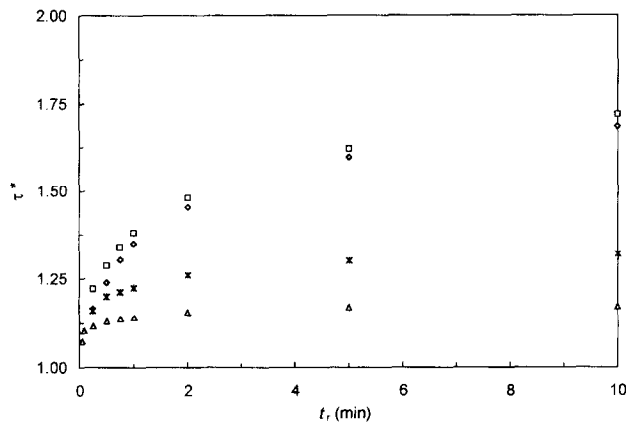


Fig. 7. Stress overshoot ratio τ^* as a function of the rest time t_r for the four systems considered at $C_p = 1.8\%$ and $T = 25^\circ\text{C}$. (Δ), HPG; (*), LMLH; (\diamond) HMLH; (\square) LMHH.

CONCLUSIONS

The application of the stepwise procedure on HPG and its long-chain derivative aqueous systems allowed an immediate distinction to be observed between the shear dependent behavior of HPG and LMLH systems and that of the other two systems considered, LMHH and HMLH. In detail, the flow properties of the former systems are quite similar to those exhibited by isotropic polymer solutions, and the popular Cross equation appears to fit the experimental data fairly well. The temperature effect can thus be discussed in terms of the corresponding variation of the Cross parameters and the relevant energy for viscous flow can be calculated by applying an Arrhenius-type equation. Moreover, the dependence of the Cross parameters η_0 and λ on polymer concentration can be properly described by simple power-law relationships, typical of concentrated entangled solutions.

In contrast, the continuous shear flow behavior of the two other systems, LMHH and HMLH, is far more complex and cannot be described by any simple rheological model. In particular, for these systems, three different flow regimes can be determined, the existence of which can be accounted for by considering both inter- and intramolecular interactions.

All these systems are characterized by time-dependent properties of the thixotropic type, which pose practical problem for the experimental determination of the equilibrium values of the corresponding shear stress. This is especially true in the shear rate range in which the catastrophic viscosity breakdown behavior is found, where times up to 1 h are necessary to reach quasi-steady stress values. By applying the on-off procedure and fitting the relevant data with a stretched exponential model we can conclude that the thixotropic recovery becomes remarkable and implies long rest times for the most concentrated hydrophobic systems with the highest degree of hydrophobization (LMHH) and molecular weight (HMLH), whereas for the HPG and LMLH systems the structural rehealing process is limited and confined within a few minutes.

ACKNOWLEDGEMENTS

The authors wish to acknowledge the Italian Ministry for University and Scientific Research for financial support (MURST 60%).

REFERENCES

- Aubry, T. & Moan, M. (1994). Rheological behavior of a hydrophobically associating water soluble polymer. *J. Rheol.*, **38**, 1681–1692.
- Ballard, M.J., Buscall, R. & Waite, F.A. (1988). The theory of shear-thickening polymer solutions. *Polymer*, **29**, 1287–1293.
- Cross, M.M. (1965). Rheology of non-Newtonian fluids: a new flow equation for pseudoplastic systems. *J. Colloid Sci.*, **20**, 417–426.
- de Gennes, P.-G. (1979). *Scaling Concepts in Polymer Physics*. Cornell University Press, Ithaca, N.Y.
- De Lorenzi, L., Molteni, G., Pricl, S. & Torriano, G. (1994). Rheological properties of water-emulsion paints containing hydrophobically-modified hydroxypropylguar as associative thickener. *Proceedings of the XXIIInd FATIPEC Congress*, Budapest, Vol. 3, pp. 67–87.
- Fonnum, G., Bakke, J. & Hansen, F.K. (1993). Associative thickeners. Part I: synthesis, rheology and aggregation behavior. *Colloid Polym. Sci.*, **271**, 380–389.
- Glass, J.E. (1989). *Polymers in Aqueous Media: Performance Through Association*, Adv. Chem. Ser. 233, ed. J.E. Glass. American Chemical Society, Washington DC.
- Jenkins, R.D., Silebi, C.A. & El-Aasser, M.S. (1991). Steady-shear and linear-viscoelastic material properties of model associative polymer solutions. *ACS Symp. Ser.*, **462**, 222–233.
- Johnson, J.F. & Porter, R.S. (1970). In *Progress in Polymer Science*, ed. A.D. Jenkins. Pergamon Press, New York, Vol. 2, Chap.4, pp. 201–256.
- Kroon, G. (1993). Associative behavior of hydrophobically modified hydroxyethylcelluloses (HMHECs) in waterborne coatings. *Prog. Org. Coatings*, **22**, 245–260.
- Landoll, L.M. (1982). Long-chain hydrophobic derivatives of cellulose. *J. Polym. Sci., Polym. Chem. Ed.*, **20**, 443–455.
- Lapasin, R. & Pricl, S. (1995). *Rheology of Industrial Polysaccharides: Theory and Applications*. Blackie Academic & Professional/Chapman & Hall, Glasgow.
- Lapasin, R., Pricl, S. & Tracanelli, P. (1991). Rheology of hydroxyethyl guar gum derivatives. *Carbohydr. Polym.*, **14**, 411–427.
- Lee, Y.-C., Baaske, D.M. & Carter, J.E. (1983). Determination of the molar substitution ratio of hydroxyethyl starches by gas chromatography. *Anal. Chem.*, **55**, 334–338.
- Mast, A.P., Prud'homme, R.K. & Glass, J.E. (1993). Behavior of low molecular weight model heur associative polymers in concentrated surfactant systems. *Langmuir*, **9**, 708–715.
- Nicora, C., Molteni, G., Cesàro, A. & Pricl, S. (1990). United States Patent No. 4960876.
- Reynolds, P.A. (1992). Association thickening of polymer latex dispersions. *Prog. Org. Coatings*, **20**, 393–409.
- Shalaby, S.W., McCormick, C.L. & Butler, G.B. (1991). *Water Soluble Polymers*, ACS Symp. Ser. 467, eds S.W. Shalaby, C.L. McCormick & G.B. Butler. American Chemical Society, Washington DC.
- Sunamoto, J., Goto, M., Iida, T., Hara, K., Saito, A. & Tomonaga, A. (1985). In *Receptor-mediated Targeting of Drugs*, eds G. Gregoriadis, G. Poste, J. Senior & A. Tranet. Plenum Press, New York, pp. 359–371.
- Sunamoto, J., Ywamoto, K., Takada, M., Yuzuriha, T. & Katayama, K. (1984). In *Polymers in Medicine*, eds E. Chiellini & P. Giusti. Plenum Press, New York, pp. 157–168.
- Witten, T.A. (1988). Associating polymers and shear-thickening. *J. Phys. France*, **49**, 1055–1063.
- Yalpani, M. (1992). *Carbohydrate and Carbohydrate Polymers: Analysis, Biotechnology, Modification, Antiviral, Biomedical and Other Applications*, ed. M. Yalpani. ATL Press, Mount Prospect.
- Yalpani, M. & Brooks, D.E. (1987). In *Industrial Polysaccharides*, eds S.S. Stivala, V. Crescenzi & I.C.M. Dea. Gordon & Breach, New York, pp. 145–156.
- Young, T.S. & Fu, E. (1991). Associative behavior of cellulosic thickeners and its implications on coating structure and rheology. *Tappi J.*, **74**, 197–207.